Vibrational Spectroscopy of Hydrogen Bonding: Origin of the Different Behavior of the C−H···O Hydrogen Bond

Weili Qian and Samuel Krimm*

Biophysics Research Division and Department of Physics, University of Michigan, Ann Arbor, Michigan 48109

Received: February 18, 2002; In Final Form: April 2, 2002

The spectroscopic behavior of the C−H···O hydrogen bond is generally opposite to that of typical (e.g., O−H···O and N−H···O) hydrogen bonds: the C−H stretching frequency is blue-shifted and the infrared band intensity decreases on hydrogen bonding. We show that this can be understood on the basis of the dynamic properties of the donor group, in particular the force on the bond resulting from the interaction of the external electric field created by the acceptor atom with the permanent and induced dipole derivatives of the X−H bond: when the field and dipole derivative are parallel, as in the case of O−H···O, the bond lengthens, and red shift and intensity increases result; when the field and dipole derivative are antiparallel, as in the case of C−H···O, the bond shortens and blue shift results with the possibility of intensity decrease. We demonstrate these properties in an ab initio and perturbation study of cis formic acid in an Onsager reaction field. This analysis provides the basis for a more general understanding of the intermolecular electrical interactions that are the underlying impetus for the formation and properties of hydrogen bonds.

Introduction

Despite an early proposal that crystallographic evidence supported the existence of C−H···O hydrogen bonds,[1] and the incorporation of such an attractive interaction in the modeling of the polypeptide structures of collagen[2] and polyglycine II,[3] it is only relatively recently that such evidence has been extended for small molecules[4−7] and is accumulating for proteins. In the latter connection, there is new crystallographic evidence for its presence in collagen,[8] in β-sheets,[9,10] in α-helices containing proline,[11] and between transmembrane helices.[12] This accounts for the general conviction that "sufficient indications for the importance of C−H···O hydrogen bonding...have accumulated to warrant their systematic consideration in future structural work".[13]

The vibrational spectroscopic evidence for such hydrogen bonds has been considered mixed, leading to the opinion that "...complementary spectroscopic evidence for [C−H···O] hydrogen bonding is noticeably absent."[14] This may have been due in part to the belief, fulfilled in some systems,[15] that, by analogy with the more traditional O−H···O and N−H···O bonds, the C−H stretch (s) frequency would always be red-shifted on hydrogen bonding. However, infrared studies on polyglycine II[16,17] had shown that the presence of attractive C−H···O interactions[17] in a crystal structure that had to contain antiparallel chains,[18] and in which such bonds were capable of existing,[19] led to a blue-shifted CH s band. (There was also a red-shifted CH s band of the CH_2 group, resulting at least in part from the positive sretch−stretch interaction force constant.[20] The presence of a red-shifted CH_2 bend mode, now confirmed by ab initio calculations on hydrogen-bonded formic acid dimer structures,[21] further supports this assignment.) Many recent experimental studies confirm the blue-shifted CH s modes for some systems (red shifted for others), and theoretical efforts have been concentrated on understanding the origin of this supposedly unusual behavior.

Two schools of thought have emerged in trying to explain the physical basis for blue-shifted CH s frequencies in some C−H···O hydrogen-bonded systems. In both cases it is acknowledged that the frequency shift results from the shortening of the C−H bond that occurs on hydrogen bonding, clearly indicated by the ab initio calculations. One group, represented by Hobza and co-workers, views such bonds as fundamentally different from traditional red-shifted bonds (initially terming them "anti-hydrogen bonds",[22−25] subsequently revising this to "improper blue-shifting hydrogen bonds"[26−29]). The origin of the bond shortening is attributed in part to dispersion effects, but primarily to "a two-step mechanism that involves [electron density transfer] from the proton-acceptor to the remote part of the proton donor, causing it to structurally relax, which in turn leads to a shortening of the [C−H] bond".[29] The other group, represented by Scheiner and Dannenberg and their co-workers, views such bonds as basically no different in nature from red-shifted hydrogen bonds: "The same forces are in operation in both types of H-bond: electrostatic, polarization, charge transfer, and dispersion push the hydrogen atom away from the donor [C] atom, while the exchange pulls it away from the acceptor [O]. While the former set are together slightly stronger than the exchange for a O−H···O bond, the latter very narrowly overcomes the former set in the C−H···O case. The red (blue) shift in the O−H···O (C−H···O) bond then follows naturally from this bond stretch (contraction)".[30] Whereas a blue shift is found in alkanes, a red shift occurs in alkynes,[31] and the C^{α}−H^{α} bond of amino acid residues undergoes a blue shift on bonding to water.[32] Electric fields alone, however, will lead to bond shortening[33,34] (in contrast to Scheiner's conclusion[30]), which reveals the dominant role of electrical interactions in determining the properties of hydrogen bonds.[35]

We agree that there is nothing "improper" about blue-shifted hydrogen bonds and that their shortened bond length results from the same principles that lead to lengthened bonds in the

* To whom correspondence should be addressed. E-mail: skrimm@umich.edu. FAX: 734-764-3323.

10.1021/jp020438g CCC: $22.00
Published on Web 06/19/2002

red-shifted cases. However, we are compelled to a different explanation of the origin of these effects as well as the infrared (IR) intensity changes that have been noted.[24,30] Previous studies have focused on static properties of the hydrogen-bonded system: structures, energies, electron density distributions. Molecular vibrations, and electrical forces associated with their changes, derive from dynamic properties of the system and these need to be considered explicitly to understand hydrogen bonding. Furthermore, it is desirable, insofar as possible, to avoid analyses that are method-dependent, such as energy decomposition, or model-dependent, such as charge distribution.

We proceed from a basic analysis of the electrical forces that act to lengthen or shorten a bond, and therefore treat a molecule in an electric field. (Simple charge considerations already hint at the different behaviors of C−H and O−H bonds.[21]) This avoids concerns about charge transfer and van der Waals interactions, which can be evaluated separately. We use a reaction field calculation as the source of the electric field since this can provide information on important hydrogen-bond properties, such as bond length changes, normal-mode frequency shifts, and IR intensity changes.[36−38] The molecule we study is the cis form of formic acid (i.e., $\tau(\mathrm{HOCH}) = 0$), so effects on O−H and C−H bonds in the same molecule can be compared.

Theory

In the reaction field model, the molecule is within a cavity in a continuous dielectric medium that can be polarized and which generates a reaction field that interacts with the molecule.[39] In the self-consistent reaction field model, the Hamiltonian has the general form $\hat{H} = \hat{H}^\circ + \hat{H}'$, where $\hat{H}^\circ$ is the Hamiltonian of the isolated molecule and $\hat{H}' = \hat{\rho}_\alpha G_{\alpha\beta}\langle\varphi|\hat{\rho}_\beta|\varphi\rangle$, φ being the wave function, $\hat{\rho}$ being the operator of the total charge density of the molecule, G being the reaction potential response function of the medium, and α and β being Cartesian coordinate components, with the same index indicating summation.[40] If the charge density is expanded in one-center multipoles, $\hat{\rho}$ becomes the multipole operator and the reaction field becomes a series in the electric field.[41] If only the dipolar leading term is taken, this becomes the Onsager model,[42] which, for simplicity, we use in this study.

Since the reaction field depends on the molecular dipole moment, which is determined by the wave function, the Schrödinger equation is nonlinear. For a nonlinear perturbation, there are different ways to treat $\hat{H}'$. It can be partitioned into contributions of different order in the field, and Angyan[43,44] has derived the general energy and wave function corrections, especially the energy terms for the Onsager model, which in the first three orders involve the dipole moment, polarizability, and hyperpolarizability of the isolated molecule. On the other hand, it can be treated as a linear perturbation, inserting $V_\alpha = \partial U/\partial x_\alpha = -F_\alpha = -g\mu_\alpha$ as the final reaction field,[45,46] where F_α is the electric field, U is the electric potential, x_α is an atomic Cartesian coordinate, g is a constant, and μ_α is the molecular dipole in the reaction field. We choose the latter method because it permits a clear physical picture of the origin of the forces in terms of permanent and induced dipole derivatives (which are mixed in the first approach and more difficult to analyze). In any case, the accuracy of this approach can be checked by the numerical results. Therefore, we take

$$\hat{H}' = \hat{\mu}_\alpha V_\alpha = -g\hat{\mu}_\alpha\mu_\alpha = -\frac{2(\epsilon-1)}{(2\epsilon+1)a_0^3}\hat{\mu}_\alpha\mu_\alpha$$

as in the Onsager model, where ϵ is the dielectric constant of the medium and a_0 is the radius of the spherical cavity.

Similar to a constant external field,[47] the total energy of the molecule has the form

$$W = W^0 + \mu_\alpha^0 V_\alpha - \frac{1}{2}\alpha_{\alpha\beta}^0 V_\alpha V_\beta + \frac{1}{6}\beta_{\alpha\beta\gamma}^0 V_\alpha V_\beta V_\gamma - \frac{1}{2}\mu_\alpha V_\alpha = W^0 + W^1 + W^2 + W^3 + W^4 \quad (1)$$

where W^0, $\alpha_{\alpha\beta}^0$, and $\beta_{\alpha\beta\gamma}^0$ are the energy, polarizability, and hyperpolarizability, respectively, of the isolated molecule, and the W^4 term is added to account for the work spent by the molecule to polarize the dielectric medium.[36,42] The other terms are given by

$$W^1 = \langle 0|\hat{H}'|0\rangle = V_\alpha\langle 0|\hat{\mu}_\alpha|0\rangle = V_\alpha\mu_\alpha^0$$

$$W^2 = -\sum_n{}' \frac{\langle 0|\hat{H}'|n\rangle\langle n|\hat{H}'|0\rangle}{W_n - W_0} = -V_\alpha V_\beta \sum_n{}' \frac{\langle 0|\hat{\mu}_\alpha|n\rangle\langle n|\hat{\mu}_\beta|0\rangle}{W_n - W_0} = -\frac{1}{2}\alpha_{\alpha\beta}^0 V_\alpha V_\beta$$

where

$$\alpha_{\alpha\beta}^0 = \sum_n{}' \frac{\langle 0|\hat{\mu}_\alpha|n\rangle\langle n|\hat{\mu}_\beta|0\rangle + \langle 0|\hat{\mu}_\beta|n\rangle\langle n|\hat{\mu}_\alpha|0\rangle}{W_n - W_0}$$

$$W^3 = -\sum_{nm}{}' \frac{\langle 0|\hat{H}'|n\rangle\langle n|\hat{H}'|m\rangle\langle m|\hat{H}'|0\rangle}{(W_n - W_0)(W_m - W_0)} - \langle 0|H'|0\rangle \sum_n{}' \frac{\langle 0|\hat{H}'|n\rangle\langle n|\hat{H}'|0\rangle}{W_n - W_0} = \frac{1}{3!}\beta_{\alpha\beta\gamma}^0 V_\alpha V_\beta V_\gamma$$

where

$$\beta_{\alpha\beta\gamma}^0 = P\left\{\sum_{nm}{}' \frac{\langle 0|\hat{\mu}_\alpha|n\rangle\langle n|\hat{\mu}_\beta|m\rangle\langle m|\hat{\mu}_\gamma|0\rangle}{(W_n - W_0)(W_m - W_0)} - \langle 0|\hat{\mu}_\alpha|0\rangle \sum_n{}' \frac{\langle 0|\hat{\mu}_\beta|n\rangle\langle n|\hat{\mu}_\gamma|0\rangle}{W_n - W_0}\right\}$$

and P stands for summation with respect to permutation of α, β, and γ.

The dipole moment of the molecule is defined as the derivative of the interaction energy of the isolated molecule with respect to the external electric field

$$\mu_\alpha = \frac{\partial W}{\partial V_\alpha} = \mu_\alpha^0 - \alpha_{\alpha\beta}^0 V_\beta + \frac{1}{2}\beta_{\alpha\beta\gamma}^0 V_\beta V_\gamma = \mu_\alpha^0 + \mu_\alpha^1 + \mu_\alpha^2 \quad (2)$$

Then, taking the derivative with respect to some internal coordinate r, we have

$$\frac{\partial\mu_\alpha}{\partial r} = \frac{\partial\mu_\alpha^0}{\partial r} - \frac{\partial\alpha_{\alpha\beta}^0}{\partial r}V_\beta + \frac{1}{2}\frac{\partial\beta_{\alpha\beta\gamma}^0}{\partial r}V_\beta V_\gamma - \alpha_{\alpha\beta}^0\frac{\partial V_\beta}{\partial r} + \beta_{\alpha\beta\gamma}^0\frac{\partial V_\beta}{\partial r}V_\gamma$$

Since

$$\frac{\partial V_\beta}{\partial r} = -g\frac{\partial\mu_\beta}{\partial r}$$

then

$$(-\alpha^0_{\alpha\beta} + \beta^0_{\alpha\beta\gamma}V_\gamma)\frac{\partial V_\beta}{\partial r} = -g(-\alpha^0_{\alpha\beta} + \beta^0_{\alpha\beta\gamma}V_\gamma)\frac{\partial \mu_\beta}{\partial r}$$

$$g\left(\frac{\delta_{\alpha\beta}}{g} - \alpha^0_{\alpha\beta} + \beta^0_{\alpha\beta\gamma}V_\gamma\right)\frac{\partial \mu_\beta}{\partial r} = \frac{\partial \mu^0_\alpha}{\partial r} - \frac{\partial \alpha^0_{\alpha\beta}}{\partial r}V_\beta + \frac{1}{2}\frac{\partial \beta^0_{\alpha\beta\gamma}}{\partial r}V_\beta V_\gamma = D^0_\alpha + D^1_\alpha + D^2_\alpha \quad (3)$$

From eq 3 we see that the dipole derivative depends on polarizability and hyperpolizability as well as their derivatives. The dipole derivative terms consist of a constant permanent dipole derivative,

$$D^0_\alpha = \frac{\partial \mu^0_\alpha}{\partial r}$$

an induced dipole derivative,

$$D^1_\alpha + D^2_\alpha = -\frac{\partial \alpha^0_{\alpha\beta}}{\partial r}V_\beta + \frac{1}{2}\frac{\partial \beta^0_{\alpha\beta\gamma}}{\partial r}V_\beta V_\gamma$$

and a reaction field part that we define as

$$D^3_\alpha = \frac{\partial \mu_\alpha}{\partial r} - D^0_\alpha - D^1_\alpha - D^2_\alpha.$$

To calculate the force *f*, we take the energy derivative with respect to some internal coordinate, i.e.,

$$f = -\frac{\partial W}{\partial r}$$

with

$$\frac{\partial W}{\partial r} = \left(\frac{\partial \mu^0_\alpha}{\partial r} - \frac{1}{2}\frac{\partial \alpha^0_{\alpha\beta}}{\partial r}V_\beta + \frac{1}{6}\frac{\partial \beta^0_{\alpha\beta\gamma}}{\partial r}V_\beta V_\gamma\right)V_\alpha + \left(\mu^0_\alpha - \alpha^0_{\alpha\beta}V_\beta + \frac{1}{2}\beta^0_{\alpha\beta\gamma}V_\beta V_\gamma\right)\frac{\partial V_\alpha}{\partial r} + g\mu_\alpha\frac{\partial \mu_\alpha}{\partial r}$$

$$= \frac{\partial \mu^0_\alpha}{\partial r}V_\alpha - \frac{1}{2}\frac{\partial \alpha^0_{\alpha\beta}}{\partial r}V_\alpha V_\beta + \frac{1}{6}\frac{\partial \beta^0_{\alpha\beta\gamma}}{\partial r}V_\alpha V_\beta V_\gamma = -f^1 - f^2 - f^3 \quad (4)$$

This equation already enables us to see what factors determine whether a bond lengthens or shortens under the influence of an external electric field. If *f* is positive (negative), a bond lengthening (shortening) is favored as a result of the lowering of the energy. The dominant ($-f^1$) term in eq 4 contributes a positive (negative) force when the permanent dipole derivative is parallel (antiparallel) to the external electric field ($F_\alpha = -V_\alpha$). The induced dipole derivative term ($D^1 + D^2$) always contributes a positive force (even though the hyperpolarizability term can be negative, its magnitude is smaller than the polarizability term), and thus the final value of *f* will be determined by the relative signs and values of $f^1$and $f^2 + f^3$. We see, therefore, that spectroscopic characteristics of a hydrogen-bonded group will be strongly influenced by dynamic properties of that group interacting with an external electric field.

Calculations

As noted above, our model molecule is the cis form of formic acid, i.e., C−H and O−H cis with respect to the O−C bond (see Figure 1). The advantages of using this molecule are several: all three terminal bonds can form hydrogen bonds; these conveniently designated bond directions, defined as C to H, O to H, and O═ to C (the bond direction for the other bond is taken as O− to C), are all close to parallel to the molecular dipole moment, which in the reaction field is the direction of the external electric field as well as that of the local field that would exist in a hydrogen-bonded system; and the above parallelism is maximally consistent with using the Onsager model (which would not be the case for the trans form, since its molecular dipole moment essentially perpendicular to the C−H and O−H bonds[48] would result in almost no field components along these bonds).

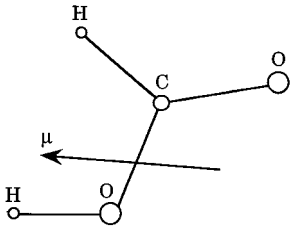

Figure 1. Optimized ab initio structure of cis form of formic acid, with indicated permanent dipole moment direction.

All calculations were done at the HF 6-311++G** level by GAUSSIAN 94.[49] Ab initio bond length changes were obtained from fully optimized structures at the different fields. By changing a_0 and/or ϵ, the initial electric field was varied between 0.00365 and 0.04336 au (a reasonable range for electric fields associated with actual hydrogen bonds). For other quantities, the comparisons are usually between ab initio values for the isolated molecule structure in the different electric fields and the values from the perturbation calculations with the reaction field using properties taken from ab initio calculations on the isolated molecule.

Since the quantities we are interested in are more convenient to use in internal than in Cartesian coordinates, all quantities in Cartesian coordinates were transformed to internal coordinates by the **A** matrix, defined as $A_{i\alpha k} = \partial x_{i\alpha}/\partial r_k$, where α is the Cartesian component and *i* and *k* are indices for the atom and internal coordinates, respectively. The **A** matrix is not uniquely defined, even in nonredundant internal coordinates, depending on the definition of all coordinates (internal and external). However, since we are interested explicitly in internal quantities, such as normal modes and IR intensities, we have used the conventional mass-dependent **A** matrix,[50,51] which is the form implemented in GAUSSIAN 94.[52]

While dipole and polarizability derivatives can be calculated analytically, the hyperpolarizabilty derivatives had to be calculated numerically. This was done for the four bond stretch coordinates by atom displacements generated by $\Delta x_{i\alpha} = A_{i\alpha k}\Delta r_k = \Delta r_k \partial x_{i\alpha}/\partial r_k$with $\Delta r_k = \pm 0.005$ bohr. It should be noted that atom displacements are usually not limited to those forming the internal coordinate, e.g., the two atoms involved in stretching a bond: such atom displacements can be contaminated by changes in other internal coordinates. We have made sure that our derivatives involve a change in only the designated internal coordinate.

Results and Discussion

Energy and Molecular Dipole Moment. The ab initio energy of the isolated molecule structure in the initial electric field is shown in Figure 2 together with the perturbation-calculated value (and its components from eq 1) as a function of the initial electric field. We see that the perturbation treatment

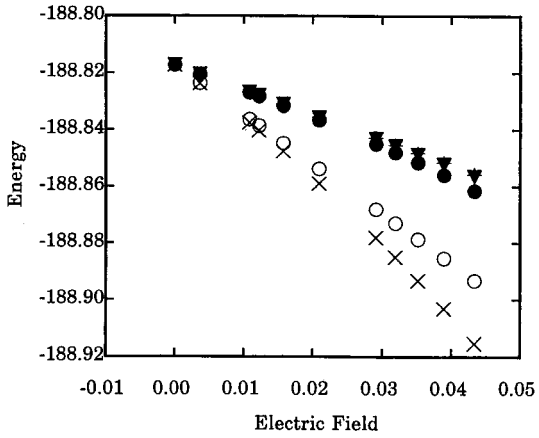

Figure 2. Ab initio energy (in au) of isolated molecule structure in reaction field (closed circles), and perturbation-calculated energy (and components, closed if overlapped) as a function of the initial electric field. O: $W^0 + W^1$. X: $W^0 + W^1 + W^2$. +: $W^0 + W^1 + W^2 + W^4$. ∇: $W^0 + W^1 + W^2 + W^4 + W^3$. (See text.)

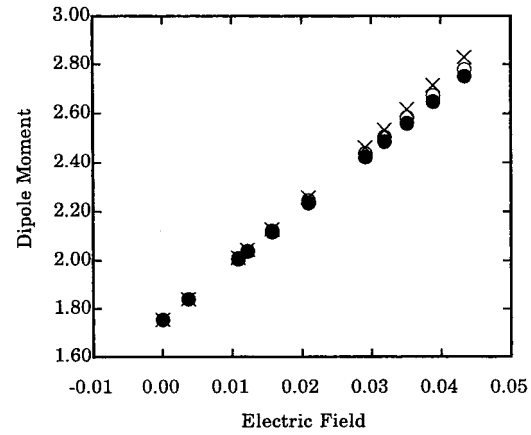

Figure 3. Ab initio molecular dipole moment (in au) of isolated molecule structure in reaction field (closed circles), and perturbation-calculated moment (and components, closed if overlapped) as a function of initial electric field. O: $\mu^0 + \mu^1$. X: $\mu^0 + \mu^1 + \mu^2$. (See text.)

is a good approximation to the correct value and that the hyperpolarizability contribution is essentially negligible. The molecular dipole moment, given by eq 2, is also well reproduced, as shown in Figure 3. Thus, the perturbation treatment can be expected to give a good representation of the dynamic properties of the molecule. It is worth noting that, while increasing dipole moment and decreasing energy are natural consequences of the polarization of the molecule in the increasing electric field, it should also not be surprising that the electron distribution within the molecule will readjust in response to the enforced change in dipole moment. And of course, in the electric field of an actual C−H···O hydrogen bond, this could lead to an enhanced electron density in "the remote part of the proton donor".[29]

Initial Forces and Bond Lengths. It is instructive to first examine how the structure responds to the initial force that it experiences in the reaction field. This force is calculated by eq 4, from properties of the isolated molecule, and the final structure is obtained from the fully optimized ab initio calculation in the reaction field. We would expect these to be well correlated, in that the direction of the force with respect to the bond direction should indicate whether the bond tends to lengthen or shorten, even though the readjustment of the initial molecular structure in response to the reaction field (which depends on many internal properties of the molecule) cannot be predicted accurately from knowledge of the initial force alone.

In Figure 4 we present these initial forces as a function of the initial electric field (open circles) and the final bond lengths as a function of the final electric field (closed circles) for the O−H (Figure 4a), O═C (Figure 4b), C−H (Figure 4c), and O−C (Figure 4d) bonds. [Thus, an initial force of 0.0199 at an initial field of 0.04336 (both in au) leads to a final O−H bond length of 0.969 Å at a final field of 0.05241 au.] From these figures we see that the O−H and O═C bonds experience positive forces and elongate in the electric field, the length increases being proportional to the field strength, whereas the C−H and O−C bonds experience negative forces and contract in the field. While in the latter case the contraction continually increases with electric field strength, in the case of C−H the contraction reverses (similar to what was observed for the C−H bond in CH_4 in a constant external electric field[34]). The interesting questions now are what is the origin of the forces and these differences, and what accounts for the turning point in the C−H bond length.

Dipole Derivatives and Forces. As we have seen from eq 4, the initial force depends on the electric field and on the permanent and induced dipole derivatives, the latter being determined by the polarizability and hyperpolarizability derivatives of the bond. The relative signs and magnitudes of the two dipole derivatives determine the sign of the force, and therefore the tendency of a bond to lengthen or shorten. In Figure 5 we show how the component terms contribute to the total force and compare this with the ab initio value, for each of the bonds. As can be seen, the force calculated by the perturbation method, i.e., eq 4, is in excellent numerical agreement with the ab initio value throughout the chosen range of electric fields.

For the O−H (Figure 5a) and O═C (Figure 5b) bonds, the force is positive and increases with the field, leading to the expected elongation of these bonds. For the C−H (Figure 5c) and O−C (Figure 5d) bonds, the force is negative and we have seen that this leads to bond contraction. The crucial difference between these two cases is that in the former the isolated molecule ab initio dipole derivative (at both HF and MP2 levels) is found to be *parallel* to the field (thus to the O−H and O═C bond directions) whereas in the latter the dipole derivative and electric field are found to be *antiparallel*: in the case of C−H, the field is parallel to the bond direction but the dipole derivative is directed from H to C; in the case of O−C, the dipole derivative is parallel to this bond direction but the field component along the bond is antiparallel to it. In other words, the essence of the effect of the electric field interaction in hydrogen bonding is to force a change in the donor bond length. Insofar as this interaction dominates[35] (charge-transfer being a small effect[30] and van der Waals interaction generally tending to shorten bonds), we should expect subsequent changes in the molecular structure (geometrical changes, charge redistributions, etc.) to "follow" from this initial process. We do not view this as a "two-stage" event: everything readjusts simultaneously; it is only a matter of what is the initiating stimulus.

To verify the generality of this explanation, we have calculated the dipole derivative directions of C−H bonds in a number of small molecule systems in which hydrogen bonding has been studied, involving a range of C hybridization: (sp^3 C) CH_4, CH_3F, CH_2F_2, CHF_3;[30,53,54] (sp^2 C) C_2H_4;[55] (sp C) C_2H_2,[31,55] C_6H_6.[22] The results are given in Table 1. In those cases in which bond contraction, and therefore blue-shifted CH s frequencies, have been predicted, the dipole derivative is antiparallel to the bond direction, which is the usual direction

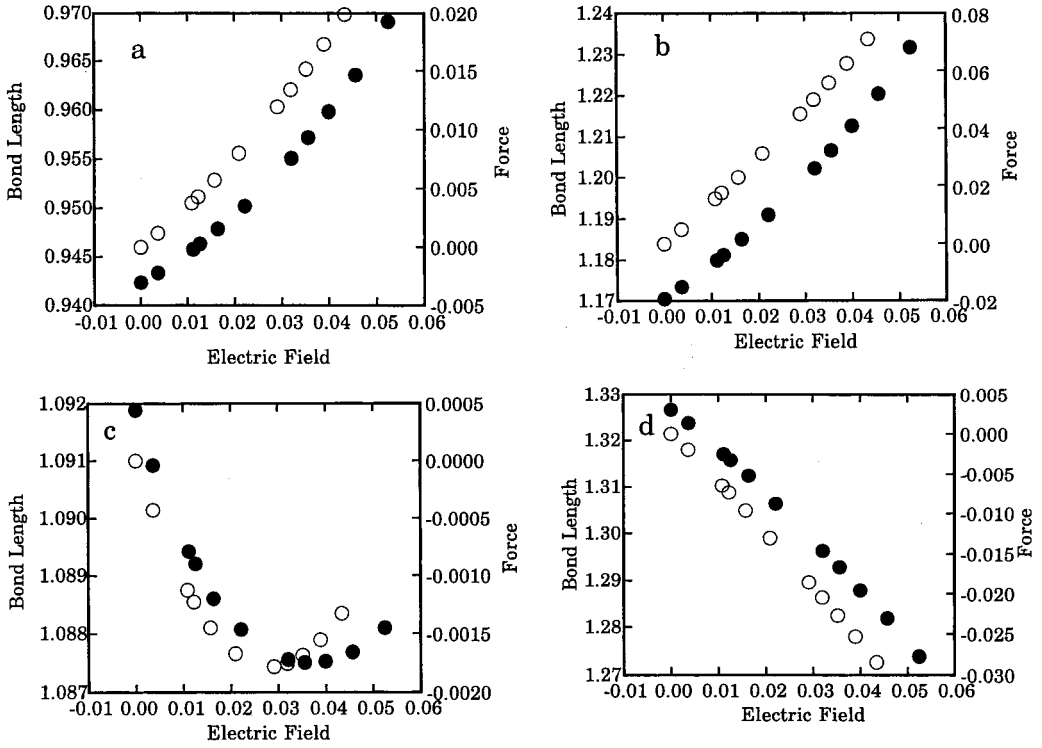

Figure 4. Final ab initio optimized bond lengths as a function of the final electric field (closed circles) and initial forces as a function of the initial electric field (open circles) for (a) O−H, (b) O═C, 9c) C−H, and (d) O−C bonds of cis formic acid. Bond lengths in angstroms, electric field in 10^{-2} au, force in au.

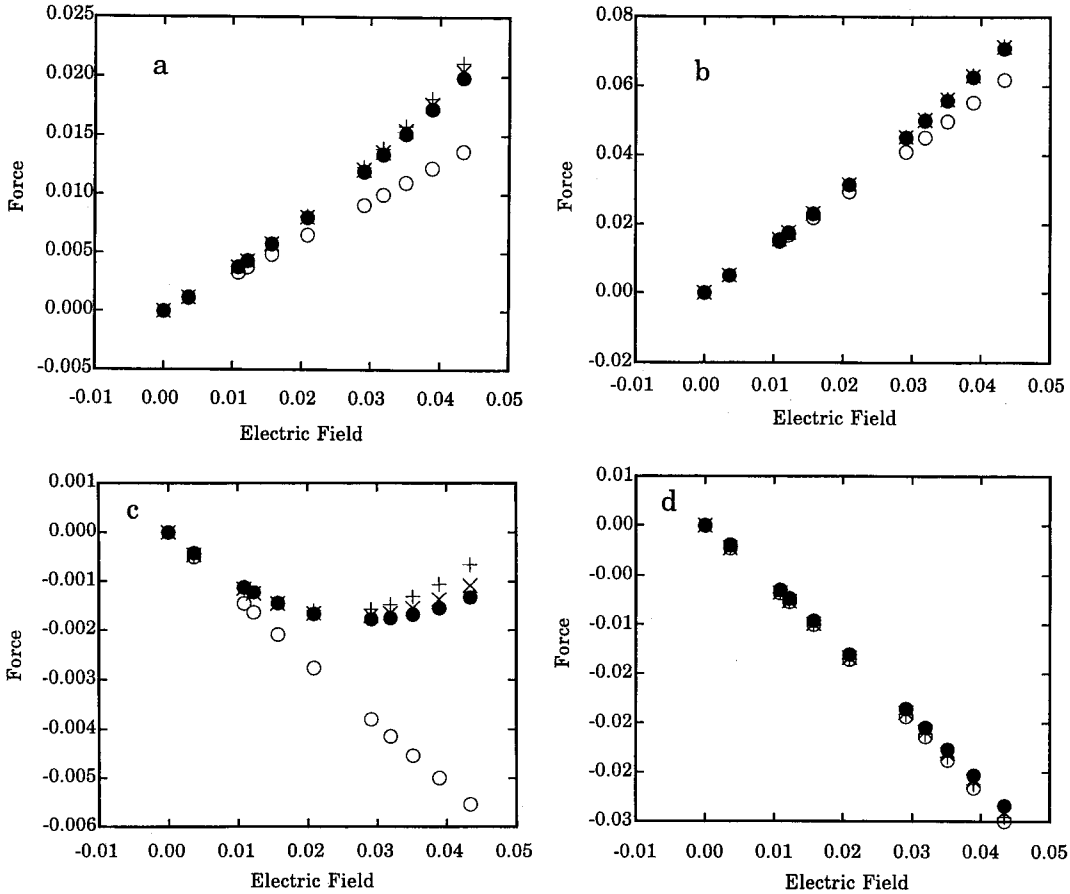

Figure 5. Initial ab initio forces (closed circles) and perturbation-calculated components and total forces as a function of initial electric field for (a) O−H, (b) O═C, (c) C−H, and (d) O−C bonds. O: f^1. X: $f^1 + f^2$. +: $f^1 + f^2 + f^3$.

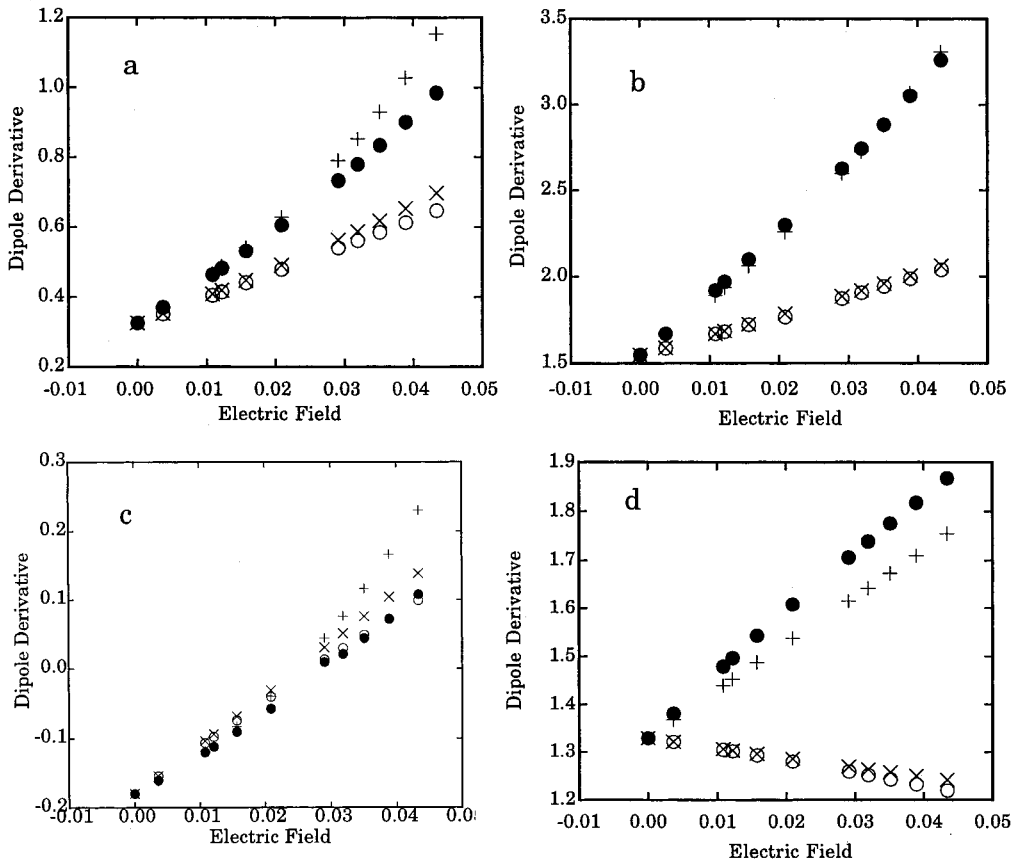

Figure 6. Final ab initio optimized dipole derivatives (closed circles) and perturbation-calculated components and total derivatives as a function of initial electric field for (a) O−H, (b) O═C, (c) C−H, and (d) O−C bonds. O: $D^\circ + D^1$. X: $D^\circ + D^1 + D^2$. +: $D^\circ + D^1 + D^2 + D^3$. (See text.)

TABLE 1: Dipole Derivative Directions in CH Bonds

molecule	$d\mu^0/dr^a$	angle[b]
HCOOH	0.18	180
CH_4	0.18	180
CH_3F	0.19	171
CH_2F_2	0.16	172
CHF_3	0.09	180
C_2H_4	0.11	180
C_2H_2	0.22	0
C_6H_6	0.12	180

[a] Dipole derivative in au. [b] Angle with respect to C−H bond direction, in degrees.

of the electric field at the bond originating from the acceptor atom (O in our case). In the one case in which a red-shift occurs, C_2H_2, the dipole derivative is parallel to the bond direction, and therefore to the field. Our argument is strongly supported by these results, which emphasize the importance of the dynamic properties of the bonds (dipole derivative, etc.) over the static (charge). Thus, although the atomic charge on C in CH_4, CH_3F, CH_2F_2, and CHF_3 varies over a wide range,[30] all the C−H bonds in these molecules undergo a contraction on hydrogen bonding because of the field-dipole derivative antiparallelism. The atomic charge representation is an incomplete description of the response of a molecule to external interactions. For example, the molecular dipole derivative cannot be reproduced by atom charges alone: charge flux (i.e. $\partial q_i/\partial r_k$, where $q_i$is the atomic charge on atom i and r_k is internal coordinate k), which is related to the dipole derivative, must be included.[56−58] (If atomic dipoles are included in the charge distribution model and atomic dipole derivatives contribute to the molecular dipole derivative, more extensive dynamic charge distribution models are possible.)

We now see the origin of the different behavior of the C−H (Figure 5c) and O−C (Figure 5d) forces with the field, which follows naturally from the relative magnitudes of the terms in eq 4. In the case C−H, f^1 is comparable to $f^2 + f^3$ and the latter becomes relatively more important at high field, causing the turnaround in f. In the case O−C, f^1 is so large in comparison to $f^2 + f^3$ that it dominates.

Dipole Derivatives and Infrared Intensities. Since the IR intensity of a band is proportional to the square of the dipole derivative of the mode, the perturbation treatment can also provide information on the behavior of this property. It has been pointed out[24,30] that, contrary to typical hydrogen bonds, C−H hydrogen bonds result in a decrease in intensity of the CH s band, although in the case of amino acids increases as well as decreases are expected.[32] Equation 3 provides a means to analyze the behavior of and contributions to the reaction field dipole derivative. (It should be noted that, although a constant external electric field will yield the same value of the force that eq 4 does for a reaction field, it will not give the same dipole derivative because of the contribution of the reaction field term in eq 3).

In Figure 6 we show a comparison of the ab initio dipole derivative of the optimized molecule in the reaction field with the value (and its components) calculated from eq 3 for the O−H (Figure 6a), O═C (Figure 6b), C−H (Figure 6c), and O−C (Figure 6d) bonds. As noted earlier, the dipole derivatives for bond directions O−H and O═C are essentially parallel to the field, leading to positive forces and bond elongation. Since the induced dipole derivative is also essentially parallel to the field (and in this case also parallel to the permanent dipole derivative), the total derivative, and therefore the IR intensity,

TABLE 2: Normal-Mode Frequencies, Infrared Intensities, Potential Energy Distributions, and Dipole Derivative Distributions for Bond Stretch Modes of cis Formic Acid

		OH s[c]		C═O s[c]		CH s[c]		C−O s[c]	
$F \times 10^2$ [a]	r[b]	PED	DDD	PED	DDD	PED	DDD	PED	DDD
0		4169[d]	*124*[e]	2041	*456*	3174	*78*	1407, 1215	*423, 42*
	OH s	100[f]	*116*[g]						
	CH s					100	*51*		
	C═O s		*8*[g]	96	*383*		*10*		*28, −6*
	C−O s			6	*97*			33, 62	*188, 69*
0.368		4153	*158*	2020	*514*	3188	*69*	1403, 1222	*474, 45*
	OH s	100	*150*						
	CH s					100	*42*		
	C═O s			95	*437*		*10*		*36, −7*
	C−O s		*10*	6	*106*			34, 62	*208, 74*
1.114		4116	*248*	1973	*638*	3211	*50*	1396, 1240	*595, 45*
	OH s	100	*240*						
	CH s					100	*25*		
	C═O s			93	*556*		*10*		*58, −9*
	C−O s		*13*	6	*124*			36, 60	*257, 79*
1.257		4107	*269*	1964	*663*	3214	*47*	1394, 1243	*621, 44*
	OH s	100	*260*						
	CH s					100	*22*		
	C═O s			93	*580*		*10*		*64, −10*
	C−O s		*14*	6	*127*			37, 60	*268, 80*
1.637		4083	*330*	1937	*728*	3223	*39*	1390, 1252	*698, 42*
	OH s	100	*321*						
	CH s					100	*15*		
	C═O s			91	*645*		*10*		*83, −11*
	C−O s			6	*135*			39, 59	*299, 79*
2.212		4044	*438*	1897	*826*	3234	*27*	1383, 1267	*840, 29*
	OH s	100	*431*						
	CH s					100	*6*		
	C═O s			88	*745*		*9*		*120, −11*
	C−O s			6	*148*			44, 54	*361, 65*
3.200		3960	*672*	1826	*956*	3245	*12*	1368, 1291	*1155, 3*
	OH s	100	*675*						
	CH s					100	*−3*		
	C═O s			80	*889*		*7*		*217, 7*
	C−O s			6	*164*			63, 37	*525, −7*
3.555		3924	*776*	1800	*982*	3247	*8*	1363, 1297	*1265, 31*
	OH s	100	*785*						
	CH s					100	*−4.9*		
	C═O s			75	*923*		*5.6*		*253, 39*
	C−O s				*167*		*0.5*	75, 25	*608, −51*
3.991		3878	*918*	1769	*990*	3249	*4*	1360, 1299	*1259, 235*
	OH s	100	*937*						
	CH s					100	*−5.4*		
	C═O s			68	*942*		*3.7*		*252, 152*
	C−O s				*171*		*0.6*	92, 7	*684, −80*
4.562		3812	*1119*	1734	*953*	3250	*1*	1365, 1288	*1015, 789*
	OH s	100	*1155*						
	CH s					100	*−3.4*		
	C═O s			57	*921*		*0.7*		*191, 414*
	C−O s				*172*		*0.8*	100, 0	*650, 17*
5.241		3714	*1431*	1695, 1501	*837, 278*	3247	*1*	1383, 1249	*749, 1571*
	OH s	99	*1502*				*−0.1*		
	CH s					99	*3.9*		
	C═O s		*−83*	40, 21	*821, 152*		*−4.7*		*148, 854*
	C−O s				*172, −3*		*1.6*	90, 7	*545, 197*

[a] Electric field, in au. [b] Internal coordinate, s = stretch. [c] Stretch mode designation. [d] Normal-mode frequencies, in cm^{-1}. [e] Normal-mode IR intensity, in km/mol. [f] Potential energy distribution, contribution ≥10. [g] Dipole derivative distribution, absolute value of contribution ≥5% of the total intensity.

increases with field strength. For the C−H bond, the situation is quite different because the permanent dipole derivative (which is small and is antiparallel to the bond direction) is antiparallel to the field, and at increasing fields the opposing induced dipole derivative reduces the total to zero and then causes it to increase in the field direction. This behavior explains how hydrogen bonding of C−H can in some cases lead to a reduction in band intensity while in others the intensity could increase. The dipole derivative of the O−C bond exhibits an apparently unusual behavior, but this is also understandable on the basis of eq 3. In this case, D° is parallel to the bond direction (therefore positive), but D^1, because the field component is antiparallel to the bond direction (see Figure 1), is negative, leading to a contributing decrease with increasing field (which is not reversed by the D^2 contribution). However, the reaction field component D^3 is very large in this case and leads to a net increasing dipole

derivative with electric field, in agreement with the ab initio trend.

Analysis of the IR intensities resulting from these dipole derivative patterns provides further insights into the actual behavior that is expected. The situation is not simply related to the dipole derivative of a bond because the normal mode can involve a mixture of internal coordinates. Nor does the usual potential energy distribution (PED) always convey the necessary information. We have pointed out that, in this regard, the dipole derivative distribution (DDD) is an important adjunct to the PED,[59] and in Table 2 we give these as well as other characteristics of the four bond stretch modes of the molecule.

As expected, the OH s and C═O s modes behave in the usual way: the frequencies decrease and the IR intensities increase with the increasing field and the resulting bond elongation. For OH s, the DDD and PED descriptions are consistent in indicating that the mode is localized in the OH bond. For C═O s, the DDD shows that the band gains a nontrivial part of its intensity from C−O s, which is not evident from the PED. In the case of CH s, the expected frequency increase and intensity decrease with increasing field is evident, and in this case the DDD shows a very significant contribution of C═O s to the intensity of the band at higher field strengths. (For the very weak bands, the quantitative results are not too meaningful, in view of the DDD contributions of other, i.e., bending, coordinates.) In the case of C−O s, the mixing pattern is even more complicated, in fact leading to significant contributions to two normal modes and a complex variation of frequency and intensity changes.

Conclusions

The fact that many CH···O hydrogen bonds exhibit a spectroscopic behavior different from that of the more typical (e.g., OH···O, N−H···O, etc.) hydrogen bonds, namely that the stretching frequency of the C−H bond is blue-shifted and its IR band intensity decreases rather than being red-shifted with an intensity increase, as in the other cases, has provided an opportunity not only to understand the basis for this difference but also to gain a deeper insight into the physical processes responsible for the hydrogen bonding interaction. We concentrate here on the electrical interaction, "a key ingredient in hydrogen bonding",[35] and show that an understanding of the dynamic, in addition to the static, properties of the donor molecule is crucial to recognizing the commonality underlying the fundamental spectroscopic results, viz., the shortening of the C−H bond versus the lengthening of O−H and N−H bonds and the decrease in its dipole derivative versus the increase in the other cases. Other interactions of course exist, but their contributions are probably not determinative: as reported by Gu et al.,[30] the effect of electron correlation on CH bond contraction is small, which is consistent with our calculation of dipole derivatives, MP2 and HF calculated dipole derivative directions for the CH bond being the same with slightly different magnitudes; charge transfer is a minor effect;[30] and van der Waals interactions, which will generally lead to contraction of the X−H bond, only enhance the C−H bond result and are not sufficient to overcome the bond elongation tendency of the electrical interactions in the other cases.

Our modeling of the electrical interaction is of a molecule in an Onsager reaction field. The molecule we study is the cis form of formic acid, which has the advantage of comparing the behavior of C−H and O−H bonds in the same molecule and in a reaction electric field (parallel to the molecular dipole moment) that has the same direction as that in actual hydrogen bonds. Because of the near parallelism of the C−H, O−H, and O═C bonds to the (constant) reaction field, the Onsager model is particularly suitable, and although improvement would probably result from using a more advanced reaction field model,[60] our perturbation treatment of the Onsager model has the advantage of revealing the underlying physical factors that contribute to the spectroscopic behavior.

The essence of our finding is that the external electric field (e.g., as created by the acceptor atom in a hydrogen bond) gives rise to a force that tends to lengthen or shorten the X−H bond depending on whether the dipole derivative of the bond is parallel or antiparallel to the field, respectively. The subsequent geometrical and spectroscopic changes in the molecule (as well as internal electronic changes) follow from this impetus. In the case of O−H, the above two quantities are always parallel; in the case of C−H, they can be antiparallel. In the case of O−H, the dipole derivative increases in the presence of a field, leading to an increased IR band intensity; in the case of C−H, the antiparallel dipole derivative, under the increasing influence of the parallel induced dipole derivative, decreases in magnitude and reverses direction as the field increases, thus leading to the possibility of a decreased IR band intensity on hydrogen bonding. These results lead to a unified view of the basic contribution made by intermolecular electrical interactions to the phenomenon of hydrogen bonding. It is interesting to note that, since the force depends on the component of the field along the bond, an angular dependence of hydrogen bonding naturally emerges.

In real molecular hydrogen bonds the electric field at the donor bond is, of course, not constant. Such a situation can be represented more accurately by a QM/MM treatment, in which it is known that a distributed multipole and polarizability model improves convergence and works well.[61] We have used the latter approach on the seven hydrogen-bonded structures of the formic acid dimer,[21] and the results are consistent with the conclusions reached here.[62]

Acknowledgment. This research was supported by NSF Grants DMR-9902727 and MCB-9903991.

References and Notes

(1) Sutor, D. J. *J. Chem. Soc.* **1963**, 1105.
(2) Ramanchandran, G. N.; Sasisekharan, V. *Biochim. Biophys. Acta* **1965**, *109*, 314.
(3) Ramanchandran, G. N.; Sasisekharan, V.; Ramakrishnan, C. *Biochim. Biophys. Acta* **1966**, *112*, 168.
(4) Taylor, R.; Kennard, O. *J. Am. Chem. Soc.* **1982**, *104*, 5063.
(5) Desiraju, G. R. *Acc. Chem. Res.* **1991**, *24*, 290.
(6) Desiraju, G. R. *Acc. Chem. Res.* **1996**, *29*, 441.
(7) Desiraju, G. R.; Steiner, T. *The Weak Hydrogen Bond*; Oxford University Press: New York, 1999.
(8) Bella, J.; Berman, H. M. *J. Mol. Biol.* **1996**, *264*, 734.
(9) Derewenda, Z. S.; Lee, L.; Derewenda, U. *J. Mol. Biol.* **1995**, *252*, 248.
(10) Fabiola, G. F.; Krishnaswamy, S.; Nagarajan, V.; Pattabhi, V.*Acta Cryst*, **1997**, *D53*, 316.
(11) Chakrabarti, P.; Chakrabarti. S. *J. Mol. Biol.* **1998**, *284*, 867.
(12) Senes, A.; Ubarretxena-Belandia, J.; Engelman, D. E. *Proc. Nat. Acad. Sci. U.S.A.* **2001**, *98*, 9056.
(13) Wahl, M. C.; Sundaralingam, M. *Trends Biochem. Sci.* **1997**, *22*, 97.
(14) Jeffrey, G. A. *J. Mol. Struct.* **1999**, *485−486*, 293.
(15) Allerhand, A.; Schleyer, P. v. R. *J. Am. Chem. Soc.* **1963**, *85*, 1715.
(16) Krimm, S.; Kuroiwa, K.; Rebane, T. *Conformation of Biopolymers;* Academic Press: London, 1967; p 439.
(17) Krimm, S.; Kuroiwa, K. *Biopolymers* **1968**, *6*, 401.
(18) Krimm, S. *Nature* **1966**, *212*, 1482.
(19) Ramanchandran, G. N.; Ramakrishnan, C.; Venkatachalam, C. M. *Conformation of Biopolymers*; Academic Press: New York, 1967; p 429.
(20) Schachtschneider, J. H.; Snyder, R. G. *Spectrochim. Acta* **1963**, *19*, 117.
(21) Qian, W.; Krimm, S. *J. Phys. Chem. A* **2001**, *105*, 5046.

(22) Hobza, P.; Spirko, V.; Selzle, H. L.; Schlag, E. W. *J. Phys. Chem. A* **1998**, *102*, 2501.
(23) Hobza, P.; Spirko, V.; Havlas, Z.; Buchhold, K.; Reimann, B.; Barth, H.-D.; Brutschy, B. *Chem. Phys. Lett.* **1999**, *299*, 180.
(24) Hobza, P.; Havlas, Z. *Chem. Phys. Lett.* **1999**, *303*, 447.
(25) Cubero, E.; Orozco, M.; Hobza, P.; Luque, F. J. *J. Phys. Chem. A* **1999**, *103*, 6394.
(26) Hobza, P.; Sponer, J.; Cubero, E.; Orozco, M.; Luque, F. J. *J. Phys. Chem. A* **2000**, *104*, 6286.
(27) Hobza, P.; Havlas, Z. *Chem. Rev.* **2000**, *100*, 4253.
(28) Hobza, P. *Phys. Chem. Chem. Phys.* **2000**, *3*, 2555.
(29) van der Veken, B. J.; Herrebout, W. A.; Szostak, R.; Shchepkin, D. N.; Havlas, Z.; Hobza, P. *J. Am. Chem. Soc.* **2001**, *123*, 12290.
(30) Gu, Y.; Kar, T.; Scheiner, S. *J. Am. Chem. Soc.* **1999**, *121*, 9411.
(31) Scheiner, S.; Grabowski, S. J.; Kar, T. *J. Phys. Chem. A* **2001**, *105*, 10607.
(32) Scheiner, S.; Kar, T.; Gu, Y. J. *J. Biol. Chem.* **2001**, *276*, 9832.
(33) Dannenberg, J. J.; Haskamp. L.; Masunov, A. *J. Phys. Chem. A* **1999**, *103*, 7083.
(34) Masunov, A.; Dannenberg, J. J.; Contreras, R. H. *J. Phys. Chem. A* **2001**, *105*, 4737.
(35) Dykstra, C. E. *Acc. Chem. Res.* **1988**, *21*, 355.
(36) Wong, M. W.; Wiberg, K. B.; Frisch, M. *J. Chem. Phys.* **1991**, *95*, 8991.
(37) Stefanovich, E. V.; Truong, T. N. *J. Chem. Phys.* **1996**, *105*, 2961.
(38) Cappelli, C.; Silva, C. O.; Tomasi, J. *J. Mol. Struct. (THEOCHEM)* **2001**, *544*, 191.
(39) Cramer, C. J.; Truhlar, D. G. *Chem. Rev.* **1999**, *99*, 2161.
(40) Constanciel, R. *Theor. Chim. Acta* **1986**, *69*, 505.
(41) Rivail, J. L.; Rinaldi, D. *Chem. Phys.* **1976**, *18*, 233.
(42) Onsager, L. *J. Am. Chem. Soc.* **1936**, *58*, 1486.
(43) Angyan, J. G.; Surjan, P. R. *Phys. Rev. A* **1991**, *44*, 2188.
(44) Angyan, J. G. *Int. J. Quantum Chem.* **1993**, *47*, 469.
(45) Luque, F. J.; Bofill, J. M.; Orozco, M. *J. Chem. Phys.* **1997**, *107*, 1293.
(46) Nielsen, C. B.; Mikkelsen, K. V.; Sauer, S. P. A. *J. Chem. Phys.* **2001**, *114*, 7753.
(47) Stone A. J. *The Theory of Intermolecular Forces*; Clarendon: Oxford, 1996; Chapter 2.
(48) Yokoyama, I.; Miwa, Y.; Machida, K. *J. Am. Chem. Soc.* **1991**, *113*, 6458.
(49) Frisch, M. J.; Trucks, G. W.; Schlegel, H. B.; Gill, P. M. W.; Johnson, B. G.; Robb, M. A.; Cheeseman, J. R.; Keith, T.; Petersson, G. A.; Montgomery, J. A.; Ragavachari, K.; Al-Laham, M. A.; Zakrzewski, V. G.; Ortiz, J. V.; Foresman, J. B.; Cioslowski, J.; Stefanov, B. B.; Nanayakkara, A.; Challacombe, M.; Peng, C. Y.; Ayala, P. Y.; Chen, W.; Wong, M. W.; Andres, J. L.; Replogle, E. S.; Gomperts, R.; Martin, R. L.; Fox, D. J.; Binkley, J. S.; Defrees, D. J.; Baker, J.; Stewart, J. P.; Head-Gordon, M.; Gonzalez, C.; Pople, J. A. GAUSSIAN 94, revision D. 4; Gaussian, Inc.: Pittsburgh, PA, 1995.
(50) Pulay, P. *Mol. Phys.* **1969**, *17*, 197.
(51) Pulay, P.; Fogarasi, G. *J. Chem. Phys.* **1992**, *96*, 2856.
(52) Peng, C.; Ayala, P.; Schlegel, H. *J. Comput. Chem.* **1996**, *17*, 49.
(53) Gu, Y.; Kar, T.; Scheiner, S. *J. Mol. Struct.* **2000**, *552*, 17.
(54) Kryachko, E. S.; Zeegers-Huyskens, T. *J. Phys. Chem. A* **2001**, *105*, 7118.
(55) Hartmann, M.; Wetmore, S. D.; Radom, L. *J. Phys. Chem. A* **2001**, *105*, 4470.
(56) Bosi, P.; Zerbi, G.; Clementi, E. *J. Chem. Phys.* **1977**, *66*, 3376.
(57) Dinur, U.; Hagler, A. T. *J. Chem. Phys.* **1989**, *91*, 2949.
(58) Qian, W.; Krimm, S. *J. Phys. Chem.* **1996**, *100*, 14602.
(59) Qian, W.; Krimm, S. *J. Phys. Chem.* **1993**, *97*, 11578.
(60) Cappelli, C.; Mennucci, B.; O. da Silva, C.; Tomasi, J. *J. Chem. Phys.* **2000**, *112*, 5382.
(61) Gordon, M. S.; Freitag, M. A.; Bandyopadhyay, P.; Jensen, J. H.; Kairys, V.; Stevens, W. J. *J. Phys. Chem. A* **2001**, *105*, 293.
(62) Qian, W.; Krimm, S. In press.